

Molecular dynamics simulation of the effect of bond flexibility on the transport properties of water

Gabriele Raabe^{1,a)} and Richard J. Sadus²

¹*Institut für Thermodynamik, Technische Universität Braunschweig, Hans-Sommer-Str. 5, 38106 Braunschweig, Germany*

²*Centre for Molecular Simulation, Swinburne University of Technology, PO Box 218, Hawthorn, Victoria 3122, Australia*

(Received 24 April 2012; accepted 17 August 2012; published online 14 September 2012)

Molecular dynamics simulations for the shear viscosity and self-diffusion coefficient of pure water were performed to investigate the effect of including intramolecular degrees of freedom in simple point charge (SPC) models over a wide range of state points. Results are reported for the flexible SPC/Fw model, its rigid SPC counterpart, and the widely used SPC/E model. The simulations covered the liquid phase from 277.15 to 363.15 K and the supercritical phase at 673.15 K and pressures up to 200 MPa. The flexibility exhibited by the SPC/Fw model results in slowing down of the dynamics. That is, it results in higher shear viscosities and lower diffusion coefficients than can be obtained from the rigid model, resulting in better agreement with experimental data. Significantly, the SPC/Fw model can be used to adequately predict the diffusion coefficients at ambient and supercritical temperatures over a wide range of pressures. © 2012 American Institute of Physics. [<http://dx.doi.org/10.1063/1.4749382>]

I. INTRODUCTION

The properties of water have a key role in many important biological, chemical, physical, and technical processes. Although the properties of aqueous systems have been extensively studied experimentally, the ability to make accurate predictions in new situations is of considerable scientific and practical value. The traditional engineering approach of developing equations of state¹ has been of limited success for water. Accurate reference equations² for pure water have been developed, but they cannot be easily extended to mixtures. Molecular simulation³ provides a useful alternative to equation of state modeling because, when used properly, it provides unambiguous information regarding the merit of the underlying model.

There are many alternative force field models for water, which reflects the difficulty of accurately predicting all the diverse properties of water. Currently, the most widely used models are rigid and variants of either the four-site⁴ transferable interaction potential (TIP4P) or the three-site simple point charge^{5,6} (SPC, SPC/E) models. Although these simple models are of great practical value and reasonably accurate at ambient conditions, the use of simplifying approximations often obscures the role of the various contributions to intermolecular interactions. This means that systematic deviations from experiment with increasing temperature are common and only certain bulk properties are adequately predicted, whereas other properties are poorly described.⁷ A major issue for most water models is that they fail to simultaneously reproduce both the diffusion coefficient (D) and the viscosity (η).⁸ In Table I, the diffusion coefficient and shear viscosities

predicted by various potentials^{12–25} at or near 298.15 K and 0.1 MPa are compared with the experimentally obtained values ($D = 2.3 \times 10^{-9} \text{ m}^2 \text{ s}^{-1}$, $\eta = 0.895 \text{ mPas}$). The calculated diffusion coefficients from different models fall within a wide range from $D = (2.08 \text{ to } 5.9) \times 10^{-9} \text{ m}^2 \text{ s}^{-1}$, representing both under and over predictions. In contrast to this, all the intermolecular potentials underestimate the shear viscosity with values ranging from 0.316 mPas to 0.886 mPas.

The TIP potentials tend to over predict the diffusion coefficient, which is most apparent for the 3 (TIP3P) or 4 (TIP4P) charge models. With regard to the shear viscosity, the TIP3P potential gives the least accurate prediction ($\eta = 0.316 \text{ mPas}$). The more recent TIP4P/2005 potential¹⁹ improves the predictions of the earlier TIP potentials, resulting in much closer agreement with experiment. The TIP4P/2005 potential also yields good results²⁶ over a range of temperatures for Poiseuille flow in nano-channels, and it is generally superior to other TIP models for a range of properties.²⁷

Most rigid SPC potentials (SPC, SPC/A, and SPC/L) also considerably overpredict D . The SPC/E model yields good results for the diffusion coefficient at ambient conditions, but the viscosity is underestimated by up to 21%.^{28–30}

Including polarizability in the force field of water is often considered necessary^{9,10,31–33} to improve the agreement with experiment for a wider range of properties and state points. Polarizable potentials approximate the effect of multi-body interactions that arise because the induced dipole of each molecule generates an electric field that affects all other molecules. The Gaussian core polarizable model (GCPM) reported by Paricaud *et al.*⁹ yields a considerable improvement for the simultaneous prediction of various properties, including the diffusion coefficient ($D = 2.263 \times 10^{-9} \text{ m}^2 \text{ s}^{-1}$). However, its ability to predict the viscosity of water remains untested. Lamoureux *et al.*¹⁰ have shown that their

^{a)} Author to whom correspondence should be addressed. Electronic mail: g.raabe@tu-bs.de.

TABLE I. Comparison with experiment for the diffusion coefficient and viscosity predicted by different intermolecular potentials at 298.15 K and 0.1 MPa.

Potential	D (10^{-9} m ² s ⁻¹)	η (mPas)	References
Expt	2.30	0.895	51, 15, 53
SPC/Fw	2.359 \pm 0.035	0.886 \pm 0.045	This work
	2.32 \pm 0.05	0.75 (300.2 K)	11
SPC/E	2.432 \pm 0.023	0.713 \pm 0.010	This work
SPC	3.861 \pm 0.030	0.410 \pm 0.010	This work
SPC/A	3.8 (300.4 K)	0.46 (300.4 K)	12
SPC/L	3.9 (300.4 K)	0.59 (299.1 K)	12
q-SPC/Fw	2.4		13
SPC(flex)	2.47 \pm 0.32 (300 K)		14
GCPM	2.26 (298 K)		9
SWM4-NDP	2.33	0.70	10
CFM	2.08 (298 K)		15
TIP3P	5.19	0.321	16, 24
TIP3P(modified)	5.9 (299.2 K)		18
TIP3P/Fs	3.53	0.51 (300.2 K)	11
TIP4P	3.29	0.494	16, 24
TIP4P/Ew	2.44 (298 K)		19
TIP4P/2005	2.08 (298 K)	0.855 (298 K)	19, 24
TIP5P	2.62	0.699	16, 24
STR/RF	3.5 (300 K)		20
COS/B2	2.6 (300 K)		20
RPOL	2.5–2.8 (298 K)		21
SSD	2.24–2.42 (298 K)		22
RWK2	3.06 (307.15 K)		23

polarizable SWM4-NDP model yields improved results for the viscosity compared to common non-polarizable models, but their simulation results ($\eta = 0.7$ mPas) still largely underestimate experimental values. Thus, although polarizable models have shown some promising results, the adequate prediction of shear viscosities and diffusion in liquid water remains a considerable challenge, which is beyond the capabilities of existing approaches. Furthermore, polarizable models are generally much more computationally demanding than non-polarizable models,^{1,7} which prohibits their use for many applications.

The introduction of bond flexibility is increasingly discussed as an indirect and computationally less expensive way of introducing polarizability effects,^{34–39} resulting in better agreement with experiment for some properties of water. The early work of Dang and Pettitt³⁷ or Toukan and Rahman³⁸ showed that flexible versions of three-site water models accurately reproduced certain aspects of the vibrational motions of neat water. López-Lemus *et al.*³⁵ have incorporated flexibility in the SPC/E model and demonstrated that the calculated surface tensions and coexisting densities of water predicted by the flexible model are closer to the experimental data than those of the rigid model. The flexible SPC/Fw model reported by Wu *et al.*¹¹ has resulted in a noticeable improvement in the accuracy of the viscosity, diffusion coefficient, and dielectric constant predicted at ambient conditions compared to the rigid SPC model. In our earlier work,³⁶ we reported that the flexible SPC/Fw model also yields a better prediction of saturation densities and the critical point than either SPC or SPC/E models and very good results were obtained for the

dielectric constant over a wide range of state points.³⁹ It is noteworthy that the best agreement with the experimental diffusion coefficient in Table I is generally observed for potentials that either include the effects of polarizability (GCPM) or bond flexibility (q-SPC/Fw, SPC(flex), SPC/Fw). The results for SPC/Fw ($D = 2.359 \times 10^{-9}$ m² s⁻¹) are almost of similar quality to those obtained from GCPM ($D = 2.263 \times 10^{-9}$ m² s⁻¹), which suggests that bond flexibility is successfully capturing the influence of polarizability on self-diffusion.

The use of bond flexibility is a promising alternative strategy for providing models that allow for the accurate simultaneous prediction of different properties. In contrast to the large amount of data at ambient conditions, intermolecular potentials are rarely tested for their ability to predict self-diffusion or shear viscosity at either high temperatures or high pressures. The ability of the SPC/Fw potential to predict diffusion coefficients has only been tested at ambient conditions.¹¹

In this work, we report molecular dynamic simulations for the SPC/Fw model for state points covering the liquid phase from 277.15 to 363.15 K and the supercritical phase at 673.15 K and pressures up to 200 MPa. For the purposes of comparison, some matching calculations were also performed with the widely used SPC/E model and the rigid SPC model. The aim of these calculations is to: (a) study systematically the effect of flexibility on the prediction of D and η for three-site simple point charge (SPC) models over a wide range of temperature and pressure including the supercritical phase; (b) determine the effect of introducing intramolecular degrees of freedom on these properties and the impact of increasing of the partial charges sites in a rigid model; and (c) gain insights into how these effects change with the thermodynamic state, i.e., with temperature and pressure.

II. THEORY

A. Water models

In the SPC⁵ model, the oxygen atom is represented as a partially charged Lennard-Jones bead, whereas the hydrogen atoms are simply represented by partial charges without any Lennard-Jones interactions. Water is modeled as a rigid molecule, with the relative positions of the three sites kept constant. The intermolecular interactions are calculated from

$$U_{inter} = \sum_i \sum_{j<i} \left\{ 4\epsilon_{ij} \left[\left(\frac{\sigma_{ij}}{r_{ij}} \right)^{12} - \left(\frac{\sigma_{ij}}{r_{ij}} \right)^6 \right] + \frac{q_i q_j}{r_{ij}} \right\}. \quad (1)$$

In their SPC/Fw model, Wu *et al.*¹¹ added molecular flexibility to the SPC model by accounting for intramolecular interactions

$$U_{intra} = \sum \frac{K_{r,OH}}{2} (r_{OH} - r_{0,OH})^2 + \sum \frac{K_{\theta,LOH}}{2} (\theta_{LHOH} - \theta_{0,LHOH})^2. \quad (2)$$

The Lennard-Jones parameters and partial charges in the SPC/Fw model remain identical to those used in the SPC model. The force constants (K_r , K_θ) and the equilibrium bond length ($r_{0,OH}$) and angle ($\theta_{0,HOH}$) were optimized to reproduce

TABLE II. Parameter values for the molecular models examined in this work.

Model	$\epsilon_{\text{OO}}/k_{\text{B}}$ (K)	σ_{OO} (Å)	q_{O} (e)	q_{H} (e)	$K_{\text{r,OH}}/k_{\text{B}}$ (K Å ⁻²)	$r_{\text{0,OH}}$ (Å)	$K_{\Theta,\text{HOH}}/k_{\text{B}}$ (K rad ⁻²)	$\Theta_{\text{0,HOH}}$ (deg)
SPC/E	78.197	3.166	-0.8476	0.4238	rigid	1.0	rigid	109.47
SPC	78.197	3.166	-0.82	0.41	rigid	1.0	rigid	109.47
SPC/Fw	78.197	3.166	-0.82	0.41	532881.6	1.012	38186.5	113.24

best the experimental bulk diffusion and dielectric constant, at ambient conditions.

By comparing simulation results from the flexible model and the corresponding rigid SPC model, we are able to investigate the effect of incorporating intramolecular degrees of freedom on the prediction of the transport properties of water. We also performed simulations on the rigid SPC/E model⁶ that uses the same geometry and Lennard-Jones parameters as the SPC model, with the addition of a self-polarization energy correction that slightly increases the partial charges. Thus, our simulations also yield insights into the effect of introducing polarization via changes to the intramolecular degrees of freedom, and increasing the partial charges. The parameters used in this work are summarized in Table II.

B. Simulation details

The molecular dynamics simulations were performed using the DL_POLY 2.20 simulation package⁴⁰ in cubic boxes consisting of $N = 400$ molecules. The cut-off radius was set to 10 Å, and standard long-range corrections to the Lennard-Jones energy and pressure were applied for all models using usual tail corrections.³ The Ewald sum was used to deal with the electrostatic interactions with a precision set to 10^{-6} to evaluate its parameters.⁴⁰ The trajectories were integrated by the velocity-Verlet algorithm.³ For each temperature and pressure, the systems were equilibrated for 2 ns in the Nosé-Hoover NpT ensemble³ to relax the system to thermodynamic equilibrium. After equilibration, ten consecutive production runs, each of 0.5 ns, were performed to determine the average density, using the standard block average technique. Time steps of $\Delta t = 0.5$ fs for the flexible model (SPC/Fw) and of $\Delta t = 1$ fs for the rigid models (SPC and SPC/E) were used. During the NpT-simulations, the coupling constants for the thermostat and the barostat were set to $\tau_{\text{T}} = 0.1$ ps and $\tau_{\text{p}} = 1.0$ ps. These simulations yielded the density of water at a given temperature and pressure.

To determine transport properties, we performed additional simulations in the Nosé-Hoover-NVT ensemble with a time step of $\Delta t = 1$ fs and a coupling constant of $\tau_{\text{T}} = 0.5$ ps. The systems were again equilibrated for 2 ns at their averaged densities from the NpT-simulations, before we performed production runs of 15 ns in the NVT ensemble, in which we saved the positions every 50 fs and the pressure tensors every 10 fs for further analysis by in-house programs.

The issue of appropriate time step is a source of uncertainty in a simulation, which also depends on the integrator used. There is an inevitable compromise between maximizing energy conservation and adequately sampling phase space and computational efficiency.⁴¹ Bond stretching vibrations are typically in the order of 10 fs but they are in the quantum-mechanical ground state,⁴² which is not accessible by classi-

cal MD. The bond angle vibration is the shortest oscillation period measured in a simulation, which is typically 13 fs. For Verlet-type integrators, it is generally accepted⁴² that 5 integration steps should be performed per harmonic oscillation period, which typically means a step size of 2–3 fs. It has been reported⁴³ that some polarizable models require 1.5–2 fs to achieve acceptable energy conservation. A time step of 2 fs is typical for a flexible potential,⁴⁴ however, values range from^{45,46} 0.25–0.5 fs to 7 fs using specialized techniques.^{42,47} Our choice of 1 fs is somewhat on the conservative side. A higher value could be used for the rigid bond potentials but using a common value for both rigid and flexible models has the benefit of being internally consistent in terms of the comparison between the intermolecular potentials.

The shear viscosity was determined by the Green-Kubo^{3,48} method of integrating the autocorrelation function of the off-diagonal elements of the viscous atomic pressure tensor $P_{\alpha\beta}$ given by

$$P_{\alpha\beta} = \left\langle \frac{1}{V} \left(\sum_i \frac{p_{i\alpha} p_{i\beta}}{m_i} + \sum_i \sum_{j>i} r_{ij\alpha} F_{ij\beta} \right) \right\rangle, \quad (3)$$

where $p_{i\alpha}$ and $p_{i\beta}$ are the α and β components of the momentum of particle i , $r_{ij\alpha}$ is the α component of the distance between the particles i and j , and $F_{ij\beta}$ is the β component of the force of their interaction. To improve the statistics, we averaged the autocorrelation functions over all independent off-diagonal tensor elements, resulting in

$$\eta = \frac{V}{3k_{\text{B}}T} \int_0^{\infty} [\langle P_{xy}(0) \cdot P_{xy}(t) \rangle + \langle P_{xz}(0) \cdot P_{xz}(t) \rangle + \langle P_{yz}(0) \cdot P_{yz}(t) \rangle] dt. \quad (4)$$

As reported elsewhere,⁴⁹ the accuracy of shear viscosity calculations can be further improved by adding additional terms. However, the benefit of the additional terms would be relatively small because Eq. (4) already includes all the independent off-diagonal tensor elements that dominate the calculation. The autocorrelation functions decay quite quickly, but then fluctuate around zero. Thus, we varied the correlation time from 3 to 10 ps to determine its influence on the resulting viscosity. We found a correlation time of 4 ps was sufficient to give viscosities that agree with results of higher correlation times within their range of uncertainties.

The self-diffusion coefficient D was determined from the Einstein relation^{3,48} as the mean-square displacement along the trajectory of a particle

$$D = \lim_{t \rightarrow \infty} \frac{\langle |r(t) - r(0)|^2 \rangle}{6t}. \quad (5)$$

As the diffusion coefficient is a single particle property, we averaged it over all particles to improve the statistics.

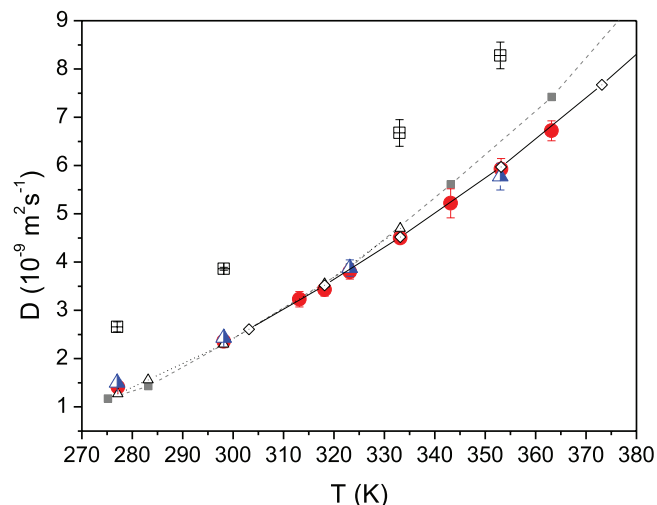


FIG. 1. The self-diffusion coefficient D of water in the liquid phase at 0.1 MPa as a function of temperature. Comparison of results from molecular dynamics simulations for the SPC/Fw (red ●), SPC/E (blue ▲), and the SPC (■) model with experimental data from Krynicky *et al.*⁵⁰ (gray ■), Harris and Woolf⁵¹ (gray ▲), and Yoshida *et al.*⁵² (◇).

Ensemble averages for the transport properties and their standard deviations were determined by dividing the analysis of the 15 ns trajectory into ten blocks.

III. RESULTS AND DISCUSSION

The simulation results using the different force field models to predict the self-diffusion coefficients (D) and the shear viscosities (η) of water in the liquid phase and in the supercritical region at 673.15 K are depicted in Figs. 1–4. The numerical simulation results in comparison with experimental data^{50–56} are also summarized in Tables II–IV.

Prior to examining the different models over a wide range of temperatures and pressures, we checked the reliability of our simulations by comparing our results with correspond-

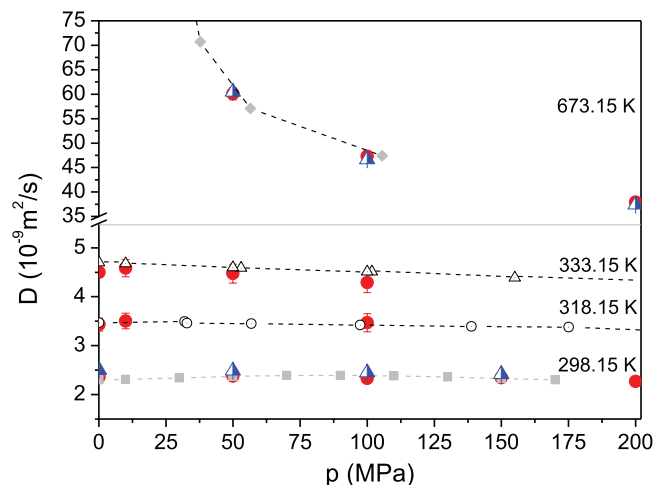


FIG. 2. The self-diffusion coefficient D of water in the liquid phase at 298.15 K, 318.15 K, and 353.5 K and in the supercritical state at 673.15 K at pressures up to 200 MPa. Comparison of results from molecular dynamics simulations for the SPC/Fw (red ●) and the SPC/E (blue ▲) model with experimental data from Krynicky *et al.*⁵⁰ (gray ■), Woolf⁵³ (gray ○), Harris and Woolf⁵¹ (gray ▲), and Lamb *et al.*⁵⁴ (gray ◆).

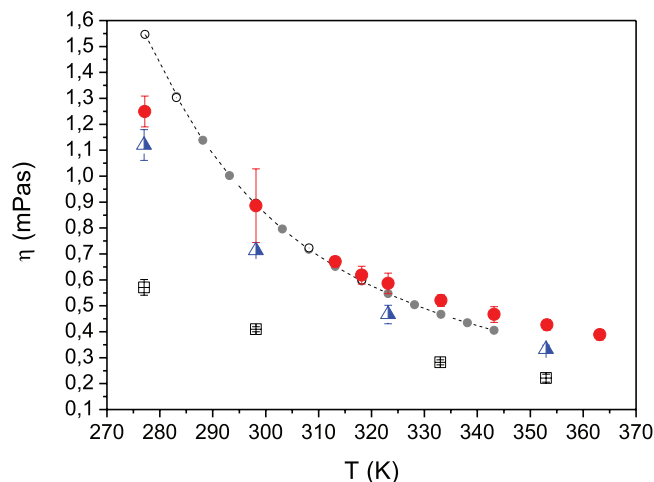


FIG. 3. Shear viscosity as a function of temperature at ambient pressure. Comparison of the results of molecular dynamics simulations for the SPC/Fw (red ●), SPC/E (blue ▲), and the SPC (■) model with experimental data from Woolf⁵³ (gray ○), and Kestin *et al.*⁵⁵ (gray ■).

ing data from the literature at 298.15 K and 0.1 MPa. For all models, there is a good agreement of our simulation results for the density ρ and the diffusion coefficient D and the data reported by Wu *et al.*¹¹ However, we note that the value of the shear viscosity at 0.1 MPa (0.75 mPas at 300.2 K), for the SPC/Fw potential reported by Wu *et al.* using an alternative to the Green-Kubo method, is lower than our calculation (0.886 mPas at 298.15 K). This can be at least partly attributed to differences in the accuracy of the simulation methods and simulation settings such as cut-off values and run length. Wu *et al.*¹¹ did not report the uncertainties for the shear viscosity calculations.

A. Self-diffusion

Figure 1 shows the self-diffusion coefficient predicted by different models at ambient pressure as a function of temperature. The comparison with the experimental data reveals that

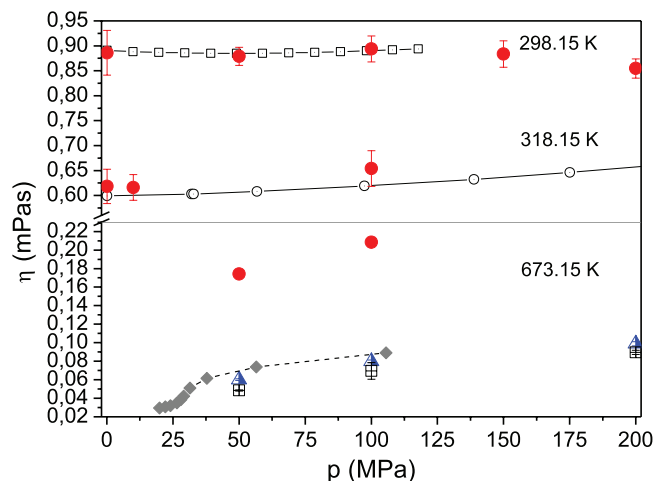


FIG. 4. The shear viscosities η of water in the liquid phase at 298.15 K and 318.15 K, and in the supercritical state at 673.15 K and pressures up to 200 MPa. Comparison of results from molecular dynamics simulations for the SPC/Fw (red ●), SPC/E (blue ▲), and SPC (■) model with experimental data from Tanaka *et al.*⁵⁶ (gray ■), Woolf⁵³ (gray ○), and Lamb *et al.*⁵⁴ (gray ◆).

TABLE III. Experimental data^{50–53,55} and molecular simulation results for the diffusion coefficient and shear viscosity in liquid water predicted by the SPC/Fw, SPC/E, and SPC models at different temperatures and 0.1 MPa. The values in brackets represent the standard deviations.

T(K)	Diffusion coefficient ($10^{-9} \text{ m}^2\text{s}^{-1}$)				Shear viscosity (mPas)			
	Expt	SPC/Fw	SPC/E	SPC	Expt	SPC/Fw	SPC/E	SPC
277.15	1.27 ^a	1.410(0.047)	1.502(0.060)	2.659(0.103)	1.546 ^b	1.249(0.06)	1.120(0.059)	0.571(0.030)
298.15	2.30 ^a	2.359(0.035)	2.432(0.023)	3.861(0.030)	0.895 ^b	0.886(0.142)	0.714(0.010)	0.410(0.010)
313.15		3.229(0.158)			0.652 ^c	0.670(0.020)		
318.15	3.55 ^a	3.431(0.134)			0.599 ^b	0.618(0.034)		
	3.52 ^d							
323.15	3.89 ^e	3.797(0.150)	3.878(0.169)		0.547 ^c	0.587(0.040)	0.466(0.036)	
333.15	4.70 ^a				0.467 ^c	0.520(0.023)		
	4.52 ^d	4.500(0.094)		6.675(0.275)				0.282(0.010)
343.15	5.61 ^e	5.218(0.302)			0.405 ^c	0.467(0.030)		
353.15	5.97 ^d	5.927(0.220)	5.770(0.277)	8.281(0.276)		0.426(0.020)	0.332(0.016)	0.221(0.016)
363.15	7.42 ^e	6.720(0.205)				0.389(0.021)		

^aHarris and Woolf.⁵¹^bWoolf.⁵³^cKestin *et al.*⁵⁵^dYoshida *et al.*⁵²^eKrynicky *et al.*⁵⁰

the SPC model largely over predicts the self-diffusion coefficient of liquid water. For example, the experimental value reported by Harris and Woolf⁵¹ at 298 K is over-estimated by approximately 68%. Both, the introduction of the self-polarization energy correction in the SPC/E model and of intramolecular degrees of freedom in the SPC/Fw model reduce the self-diffusion coefficients remarkably. The simulation results for the SPC/E and the SPC/Fw model are very similar and reproduce the experimental data up to 333 K very well. This is also true for elevated pressures as illustrated by Fig. 2.

It should be noted that although there is good agreement between different sources of experimental data for

the self-diffusion coefficient at low temperatures, significant discrepancies emerge at higher temperatures. These experimental discrepancies are evident in Fig. 1. For example, at 363 K the interpolated diffusion coefficient reported by Yoshida *et al.*⁵² is 8% smaller than the experimental value of Krynicky *et al.*⁵⁰ The simulation results obtained from the SPC/Fw and the SPC/E models are close to the experimental data of Yoshida *et al.*,⁵² but understandably underestimate the diffusion coefficients reported by Krynicky *et al.*⁵⁰ In the supercritical region (Fig. 2), both models again yield good estimates of the diffusion coefficients, which are in good agreement with experimental values reported by Lamb *et al.*⁵⁴

TABLE IV. Experimental data^{50,51,53,54,56} and molecular simulation results for the diffusion coefficient and shear viscosity in liquid water predicted by the SPC/Fw model at different temperatures and pressures up to 200 MPa. The values in brackets represent the standard deviations.

T/K	p/MPa	Diffusion coefficient ($10^{-9} \text{ m}^2 \text{ s}^{-1}$)		Shear viscosity (mPas)	
		Expt	SPC/Fw	Expt	SPC/Fw
298.15	0.1	2.30 ^a	2.359(0.035)	0.891 ^b	0.886(0.142)
	50	2.37 ^a	2.378(0.027)	0.885 ^b	0.879(0.018)
	100	2.38 ^a	2.328(0.045)	0.890 ^b	0.894(0.026)
	150	2.33 ^a	2.344(0.041)		0.884(0.027)
	200		2.269(0.011)		0.855(0.019)
318.15	0.1	3.47 ^c	3.432(0.134)	0.599 ^c	0.618(0.034)
	10	3.48 ^{c*}	3.502(0.160)	0.600 ^{c*}	0.616(0.026)
	100	3.42 ^{c*}	3.468(0.187)	0.620 ^{c*}	0.654(0.035)
333.15	0.1	4.70 ^d	4.499(0.094)		0.520(0.023)
	10	4.68 ^{d*}	4.584(0.177)		0.536(0.038)
	50	4.60 ^{d*}	4.472(0.193)		0.531(0.038)
	100	4.51 ^{d*}	4.290(0.208)		0.519(0.303)
673.15	50	61.83 ^{e*}	60.086(1.222)	0.069 ^{e*}	0.174(0.033)
	100	48.51 ^{e*}	47.297(0.531)	0.087 ^{e*}	0.208(0.034)
	200		37.900(0.412)		0.250(0.052)

^aKrynicky *et al.*⁵⁰^bTanaka *et al.*⁵⁶^cWoolf⁵³ (*interpolated).^dHarris and Woolf⁵¹ (*interpolated).^eLamb *et al.*⁵⁴ (*interpolated).

TABLE V. Equilibrium bond lengths r_{OH} , bond angles Θ_{HOH} , and dipole moment μ of the flexible model SPC/Fw in the liquid phase at ambient pressure (0.1 MPa) and in the supercritical fluid. Values in parentheses denote standard deviations.

	r_{OH} (Å)	Θ_{HOH} (deg)	μ (D)
298.15 K, 0.1 MPa	1.0310 (2×10^{-5})	107.700 (0.002)	2.39388 (9×10^{-5})
313.15 K, 0.1 MPa	1.03074 (2×10^{-5})	107.746 (0.002)	2.39165 (9×10^{-5})
333.15 K, 0.1 MPa	1.02992 (1×10^{-5})	107.799 (0.001)	2.38815 (7×10^{-4})
353.15 K, 0.1 MPa	1.02961 (1×10^{-5})	107.864 (0.001)	2.38544 (6×10^{-5})
673.15 K, 50 MPa	1.0228 (4×10^{-6})	109.30 (0.001)	2.32690 (5×10^{-5})

B. Shear viscosities

The predictions of the various models for shear viscosities at ambient conditions are compared with experimental data in Fig. 3. It is apparent from this comparison that the rigid SPC model considerably underestimates shear viscosities. The introduction of flexibility to the SPC model in the SPC/Fw model has a similar effect as the increase of the partial charges in the rigid SPC/E model, namely to yield significantly higher viscosities. However, in contrast to the very similar results obtained for the self-diffusion coefficients, the SPC/E and SPC/Fw models yield remarkably different results for the shear viscosity. For example, at 298 K and 0.1 MPa, the deviation between the diffusion coefficients of the two models is only about 3%, whereas their predicted shear viscosities differ by 24%. At temperatures up to 323 K the SPC/E still largely underestimates the experimental viscosities. In contrast, the flexible SPC/Fw model performs well in predicting the liquid shear viscosities in the temperature range from 298.15 to 323.15 K, and also at higher pressures, as shown in Fig. 4.

At ambient temperatures, the SPC/Fw model enables a good reproduction of both the diffusion coefficient and the shear viscosity over a wide range of pressures. However, it is apparent from Fig. 3 that all models underestimate the decrease of the viscosities with increasing temperatures, i.e., they predict a too flat curve progression $\eta(T)$.

Although the SPC/Fw model shows good agreement with experimental shear viscosities at near ambient temperatures, it underestimates the shear viscosities at lower temperatures (e.g., 277 K) and increasingly overestimates them with increasing temperatures. For the SPC/E model, which underestimates the shear viscosity at ambient temperatures, the deviations from experimental values decrease with increasing temperatures. Additionally, the results for the SPC and the SPC/E models gradually meet with increasing temperatures and especially in the supercritical region as shown in Fig. 4. From this observation it can be concluded that the introduction of bond flexibility has a very pronounced influence on the prediction of the shear viscosity of water, which also differs from its effect on the diffusion coefficient.

C. Impact of flexibility

To study the impact of introducing flexibility, we have determined the values for the equilibrium O–H bond length r_{OH} , the equilibrium bond angle Θ_{HOH} and the dipole moment μ at different state points. The values are summarized in

Table V. The comparison of the values of the flexible model and the corresponding rigid SPC model ($\mu_{\text{SPC}} = 2.274$ D) shows that introducing flexibility significantly increases the molecular dipole moment. The varying values of the dipole moment of SPC/Fw (see Table V) also indicate that a flexible model allows the molecular dipole moment to change with the thermodynamic state point, and thereby mimic the change of the intermolecular interactions in response to the local environment. The results for the equilibrium geometry show that the equilibrium bond length r_{OH} of the flexible model is significantly larger than the model parameter $r_{0,\text{OH}}$, and also that of the bond length of the rigid SPC model with $r_{\text{OH}} = 1$ Å. However, the equilibrium bond angle is remarkably smaller than the model parameter $\Theta_{0,\text{HOH}}$ and the H–O–H angle of the rigid models ($\Theta_{0,\text{HOH}} = 109.47^\circ$). Both the elongation of the equilibrium O–H-bonds and the smaller equilibrium bond angles result in the larger molecular dipole moments of the flexible model compared to the rigid SPC model with the same point charges.

Wu *et al.*¹¹ reported that the diffusion coefficient is sensitive to the equilibrium length of the O–H bond, with the diffusion coefficient decreasing with the elongation of the bond length. However, comparing the results for the diffusion coefficient of the different models studied in this work, it becomes apparent that the transport properties and their dependence on the state point predicted by the flexible model depend in a more complex way on different factors, i.e., the bond length and bond angle, but also the dipole moment. The smaller diffusion coefficient and higher viscosity of the rigid SPC/E model compared to the SPC model with the same geometry is caused by its higher dipole moment ($\mu_{\text{SPC/E}} = 2.352$ D). The reduced diffusion coefficient and increased shear viscosity of the flexible model compared to its rigid SPC counterpart can be attributed to the elongated O–H bond, which in turn also results in the increased dipole moment. However, this slowing down of the dynamics with increasing bond lengths is partially compensated by their smaller bond angles compared to the rigid model. This is well illustrated by comparing the diffusion coefficient of the SPC/Fw and the SPC/E model at 298.15 K. Due to its elongated O–H-bond length and higher dipole moment, it could be expected that the SPC/Fw model would have a smaller diffusion coefficient than the SPC/E model. However, both models yield quite similar results due to the smaller equilibrium bond angle of the SPC/Fw model that increases the self-diffusion coefficient.

When the temperature increases, the diffusion coefficients predicted by the SPC/E model increase only due to

the corresponding decrease in density. For the flexible model, increasing temperature also results in smaller equilibrium bond lengths and dipole moments, which in turn cause a higher diffusivity. However, at the same time, their equilibrium bond angles expand, which slows down the motion. For the SPC/Fw model, these opposing trends seem to compensate for the diffusion coefficient, so that its change with the state point is mainly affected by the density in the same way as for the SPC/E model. Thus, both models yield very similar results over the entire range of state point studied here. The interplay of the different influences is also well shown by the results for the self-diffusion coefficient in the supercritical region at 673.15 K, where the SPC/E and SPC/Fw models give very similar results. The SPC/E and SPC/Fw models now have comparable H–O–H bond angles, which means that the effect of the elongated O–H bond of the SPC/Fw model on the diffusion coefficient is compensated by its smaller dipole moment.

In view of the observation that, because of compensating factors, the diffusion coefficient of the SPC/E and the flexible models approach each other with increasing temperature, it might be considered surprising that the differences in the predicted shear viscosity increase at higher temperatures. This implies that viscosity is more sensitive to changes in the equilibrium bond angle than diffusion. Again, the decrease of the viscosity of the rigid SPC/E model with rising temperatures is only caused by decreasing densities. For the flexible model, apart from the density effect, decreasing equilibrium bond length and dipole moment with increasing temperatures reduce the shear viscosity, so that it should give similar or even smaller shear viscosities than the SPC/E model. The fact that the SPC/Fw model instead largely overestimates the viscosities at higher temperatures indicates that the model is sensitive to the slowing down of the dynamics with expanding bond angles.

IV. CONCLUSIONS

We have performed molecular dynamics simulations of the flexible SPC/Fw models in comparison with their rigid counterpart, the SPC model, and the widely used SPC/E model. In general, the introduction of intramolecular degrees of freedom in the SPC/Fw model has a similar effect as the increase of the partial charges in the rigid SPC/E model, i.e., higher shear viscosities and lower diffusion coefficients are predicted compared with the results from the SPC model.

Significantly, the SPC/Fw model can be used to adequately predict the diffusion coefficients at both ambient and supercritical temperatures over a wide range of pressures. Although the SPC/Fw model provides a good prediction of the shear viscosities at ambient temperatures, it largely overestimates them at higher temperatures. It can be observed that all models studied in this work significantly underestimate the decrease of the viscosities of water with increasing temperatures.

We found that the flexible model shows elongated equilibrium O–H-bonds compared to the rigid model, whereas the equilibrium bond angle decreases below the value of the SPC or SPC/E model. Both effects result in higher molecu-

lar dipole moments of the SPC/Fw model compared to the SPC model with the same point charges. When the temperature is increased (i.e., at decreasing densities), the O–H-bonds of the flexible model slightly contract but remain elongated compared to the rigid models. In contrast, the equilibrium H–O–H bond angles increase with temperature. The changes in geometry in response to the thermodynamic state point allow the molecular dipole moment to vary. The dynamics of the systems are affected by interplay of both changes in the equilibrium bond length and dipole moment, and changes in the bond angle. For the diffusion coefficient, the opposing effects of decreasing bond length and increasing H–O–H angle seems to counteract each other. The overestimated viscosities at higher temperatures might be attributed to the sensitivity of the viscosity to the slowing down of the dynamics with increasing bond angles.

- ¹Y. S. Wei and R. J. Sadus, *AIChE J.* **46**, 169 (2000).
- ²A. Pruß and W. Wagner, *J. Phys. Chem. Ref. Data* **31**, 387 (2002).
- ³R. J. Sadus, *Molecular Simulation of Fluids: Theory, Algorithms and Object-Oriented* (Elsevier, Amsterdam, 1999).
- ⁴W. L. Jorgensen, J. Chandrasekhar, J. D. Madura, R. W. Impey, and M. L. Klein, *J. Chem. Phys.* **79**, 926–935 (1983).
- ⁵H. J. C. Berendsen, J. P. M. Postma, W. F. van Gunsteren, and J. Hermans, in *Intermolecular Forces*, edited by B. Pullman (Reidel, Dordrecht, 1981).
- ⁶H. J. C. Berendsen, J. R. Grigera, and T. P. Straatsma, *J. Phys. Chem.* **91**, 6269 (1987).
- ⁷S. Iuchi, S. Izvekov, and G. A. Voth, *J. Chem. Phys.* **126**, 124505 (2007).
- ⁸U. Balucani, J. P. Brodholt, P. Jedlovsky, and R. Vallauri, *Phys. Rev. E* **62**, 2971 (2000).
- ⁹P. Paricaud, M. Prědota, A. A. Chialvo, and P. T. Cummings, *J. Chem. Phys.* **122**, 244511 (2005).
- ¹⁰G. Lamoureux, E. Harder, I. V. Vorobyov, B. Roux, and A. D. MacKerell, Jr., *J. Chem. Phys. Lett.* **418**, 245 (2006).
- ¹¹Y. Wu, H. L. Tepper, and G. A. Voth, *J. Chem. Phys.* **124**, 024503 (2006).
- ¹²A. Glättli, X. Daura, and W. F. van Gunsteren, *J. Chem. Phys.* **116**, 9811 (2002).
- ¹³F. Paesani, W. Zhang, D. A. Case, T. E. Cheatham III, and G. A. Voth, *J. Chem. Phys.* **125**, 184507 (2006).
- ¹⁴D. M. Ferguson, *J. Comput. Chem.* **16**, 501 (1995).
- ¹⁵F. Bresme, *J. Chem. Phys.* **115**, 7564 (2001).
- ¹⁶M. W. Mahoney and W. L. Jorgensen, *J. Chem. Phys.* **114**, 363 (2001).
- ¹⁷Y. Song and L. L. Dai, *Mol. Simul.* **36**, 560 (2010).
- ¹⁸P. Mark and L. Nilsson, *J. Phys. Chem. A* **105**, 9954 (2001).
- ¹⁹J. L. F. Abascal and C. Vega, *J. Chem. Phys.* **123**, 234505 (2005).
- ²⁰H. Yu, T. Hansson, and W. F. van Gunsteren, *J. Chem. Phys.* **118**, 221 (2003).
- ²¹S. Koneshan, J. C. Rasaiah, and L. X. Dang, *J. Chem. Phys.* **114**, 7544 (2001).
- ²²A. Chandra and I. Ichiye, *J. Chem. Phys.* **111**, 2701 (1999).
- ²³Z. Duan, N. Møller, and J. H. Weare, *Geochim. Cosmochim. Acta* **59**, 3273 (1995).
- ²⁴M. A. González and J. L. F. Abascal, *J. Chem. Phys.* **132**, 096101 (2010).
- ²⁵R. Mills, *J. Phys. Chem.* **77**, 685 (1973).
- ²⁶A. P. Markesteijn, R. Hartkamp, S. Luding, and J. Westerweel, *J. Chem. Phys.* **136**, 134104 (2012).
- ²⁷C. Vega, J. L. F. Abascal, M. M. Conde, and J. L. Aragonés, *Faraday Discuss.* **141**, 251 (2009).
- ²⁸S. Balasubramanian, C. J. Mundy, and M. L. Klein, *J. Chem. Phys.* **105**, 11190 (1996).
- ²⁹D. R. Wheeler and R. L. Rowley, *Mol. Phys.* **94**, 555–564 (1998).
- ³⁰G. Delgado-Barrio, R. Prosmi, P. Villarreal, G. Winter, J. S. Medina, B. González, J. V. Gomez, P. S. Sangrá, J. J. Santana, and M. E. Torres, in *Frontiers in Quantum Systems in Chemistry and Physics*, edited by S. Wilson, P. J. Grout, G. Delgado-Barrio, J. Maruani, and P. Piecuch (Springer, Berlin, 2008), Vol. 18, p. 351.
- ³¹I. M. Svishchev, P. G. Kusalik, J. Wang, and R. J. Boyd, *J. Chem. Phys.* **105**, 4742 (1996).
- ³²I. M. Svishchev and T. M. Hayward, *J. Chem. Phys.* **111**, 9034 (1999).
- ³³J. Li, Z. Zhou, and R. J. Sadus, *J. Chem. Phys.* **127**, 154509 (2007).

- ³⁴T. I. Mizan, P. E. Savage, and R. M. Ziff, *J. Comp. Chem.* **17**, 1757 (1996).
- ³⁵J. López-Lemus, G. A. Chapela, and J. Alejandro, *J. Chem. Phys.* **128**, 174703 (2008).
- ³⁶G. Raabe and R. J. Sadus, *J. Chem. Phys.* **126**, 044701 (2007).
- ³⁷L. X. Dang and B. M. Pettitt, *J. Phys. Chem.* **91**, 3349 (1987).
- ³⁸K. Toukan and A. Rahman, *Phys. Rev. B* **31**, 2643 (1985).
- ³⁹G. Raabe and R. J. Sadus, *J. Chem. Phys.* **134**, 234501 (2011).
- ⁴⁰W. Smith and T. R. Forester, The DL_POLY Molecular Simulation Package, see http://www.cse.clrc.ac.uk/msi/software/DL_POLY.
- ⁴¹D. Fincham, *Comp. Phys. Commun.* **40**, 263 (1986).
- ⁴²K. A. Feenstra, B. Hess, and H. J. C. Berendsen, *J. Comput. Chem.* **20**, 786 (1999).
- ⁴³G. Ruocco and M. Sampoli, *Mol. Phys.* **82**, 875 (1994).
- ⁴⁴M. Levitt, M. Hirshberg, R. Sharon, K. E. Laidig, and V. Daggett, *J. Phys. Chem. B* **101**, 5051 (1999).
- ⁴⁵A. K. Mazur, *J. Comp. Phys.* **136**, 354 (1997).
- ⁴⁶M. Praprotnik and D. Janežič, *J. Chem. Phys.* **122**, 174103 (2005).
- ⁴⁷J. A. Izaguirre, S. Reich, and R. D. Skeel, *J. Chem. Phys.* **110**, 9853 (1999).
- ⁴⁸M. P. Allen and D. J. Tildesley, *Computer Simulation of Liquids* (Clarendon, Oxford, 1987).
- ⁴⁹P. J. Daivis and D. J. Evans, *J. Chem. Phys.* **100**, 541 (1994).
- ⁵⁰K. Krynicki, C. D. Green, and D. W. Sawyer, *Faraday Discuss. Chem. Soc.* **66**, 199 (1978).
- ⁵¹K. R. Harris and L. A. Woolf, *J.C.S. Faraday I* **76**, 377 (1980).
- ⁵²K. Yoshida, C. Wakai, N. Matubayaski, and M. Nakahara, *J. Chem. Phys.* **123**, 164506 (2005).
- ⁵³L. A. Woolf, *J. Chem. Soc., Faraday Trans. 1* **71**, 784 (1975).
- ⁵⁴W. J. Lamb, G. A. Hoffman, and J. Jonas, *J. Chem. Phys.* **74**, 6875 (1981).
- ⁵⁵J. Kestin, M. Sokolov, and W. A. Wakeham, *J. Phys. Chem. Ref. Data* **7**, 941–948 (1978).
- ⁵⁶Y. Tanaka, Y. Matsuda, H. Fujiwara, H. Kuboty, and T. Makita, *Int. J. Thermophys.* **8**, 147 (1987).